Superabsorption of acoustic waves with bubble metascreens

Valentin Leroy,[1] Anatoliy Strybulevych,[2] Maxime Lanoy,[3,1] Fabrice Lemoult,[2,3] Arnaud Tourin,[3] and John H. Page[2]

[1]*Laboratoire Matière et Systèmes Complexes, Université Paris-Diderot, CNRS (UMR 7057), Paris, France*
[2]*Department of Physics and Astronomy, University of Manitoba, Winnipeg, Canada*
[3]*ESPCI Paris Tech, PSL Research University, CNRS, Institut Langevin, F-75005 Paris, France*

A bubble metascreen, i.e., a single layer of gas inclusions in a soft solid, can be modeled as an acoustic open resonator, whose behavior is well captured by a simple analytical expression. We show that by tuning the parameters of the metascreen, acoustic superabsorption can be achieved over a broad frequency range, which is confirmed by finite element simulations and experiments. Bubble metascreens can thus be used as ultrathin coatings for turning acoustic reflectors into perfect absorbers.

PACS number(s): 43.20.+g, 43.30.+m, 78.67.Pt

Waves carry energy. In many situations, absorbing as much as possible of this energy is desirable. One may want, for instance, to convert the mechanical energy of an ocean swell into electrical energy, or to detect very weak electromagnetic waves, or just to limit the nuisance due to acoustic noise. Absorbing all the energy of an incoming wave requires that two problems be tackled: Not only must the transmission be reduced to zero, but the reflection as well. This means that a very dissipative medium that is not impedance matched to the environment is not a solution: The incoming wave will reflect from it without losing much of its energy. An absorber thus consists of a lossy material (to reduce transmission) with an impedance close to that of the environment (to reduce reflection). Perfect absorption can be easily achieved if the thickness of the material is large enough for all the energy to be dissipated. However, in practice, one often wants the absorber to be as small and light as possible, requiring a thin piece of material. Minimizing the thickness of the absorber and, ideally, reaching a subwavelength structure, is the issue of superabsorption.

Metamaterials are the key to achieve superabsorption. These materials are made of "metamolecules", i.e., local resonators that can couple to the incoming wave despite being small compared to the wavelength. By designing judiciously the structure of a metamaterial, one can obtain exotic properties such as negative refraction [1–4], invisibility cloaks [5–8], subwavelength focusing [9,10], or superabsorption [11–16]. Many types of resonators have been identified and investigated, from split rings for electromagnetic waves [11] to loaded membranes for acoustic waves [14,15]. Here we consider a particularly simple resonator that is well known to couple strongly with waterborne acoustic waves: the gas bubble.

In this Rapid Communication, we show how a very efficient absorber of acoustic waves can be constructed from a single, deeply subwavelength layer of bubbles immersed in a soft elastic matrix. While most previous research has investigated either narrow band superabsorption of airborne sound in subwavelength metalayers, or broadband absorption for larger metastructures, we demonstrate that the ideal situation of broadband superaborption can be achieved for waterborne acoustic waves in a single metalayer that is much thinner than the wavelength. The key to the success of our approach is an *analytic* model that reveals directly how the local structure of the metamaterial can be tuned to optimize the absorption.

We validate the model predictions with simulations and ultrasonic experiments, which demonstrate peak absorption greater than 97% and broadband absorption greater than 91% for frequencies that extend over a factor of 2 in range. At the absorption peak, the experiments show that the reflectance of our optimized metastructure is almost zero (less than 0.2%). Our results demonstrate how anechoic coatings with optimum performance can be designed for technologically relevant applications of waterborne acoustic waves.

The structure we consider is sketched in the inset of Fig. 1: The bubble metascreen consists of a layer of gas cylinders in a soft solid, here organized on a square lattice. It has been shown that, at low frequencies, providing that the aspect ratio of the cylinders is close to unity and the shear modulus μ of the soft solid is not too high ($\mu < 10$ MPa), the cavities can be modeled as spherical bubbles of the same volume [17–19]. In particular, the cavities exhibit a low-frequency resonance, similar to the Minnaert resonance, $\omega_0 = \sqrt{(3\beta_g + 4\mu)/\rho}/a$, where β_g is the bulk modulus of the gas, ρ the density of the solid, and a the radius of the bubble [$a = (3D^2H/16)^{1/3}$, with the notations of Fig. 1's inset]. Calculating the transmission and reflection coefficients for an incident longitudinal wave on such a structure is a complicated matter. Indeed, the coupling between the cavities is too strong to be neglected, and shear waves also need to be taken into account, two factors that make numerical simulations computationally intensive [20,21]. However, a simple model was recently proposed [22] to calculate the transmission and reflection from a single layer of bubbles. It predicts that an incoming plane pressure wave $\exp[i(kx - \omega t)]$, at angular frequency ω and with wave number k, is reflected and transmitted with coefficient r and t given by

$$r = \frac{iKa}{\left(\frac{\omega_0}{\omega}\right)^2 - I - i(\delta + Ka)}, \tag{1a}$$

$$t = 1 + \frac{iKa}{\left(\frac{\omega_0}{\omega}\right)^2 - I - i(\delta + Ka)}, \tag{1b}$$

where $K = 2\pi/(kd^2)$, $I = 1 - Ka\sin(kd/\sqrt{\pi})$, and δ is the dissipative damping constant. This model has been experimentally confirmed for bubbles in a yield-stress fluid [22] and for air cylinders in an elastomer [17], in the ultrasonic frequency range. In Fig. 1, we show it also gives good agreement with simulations in the audible frequency range, for
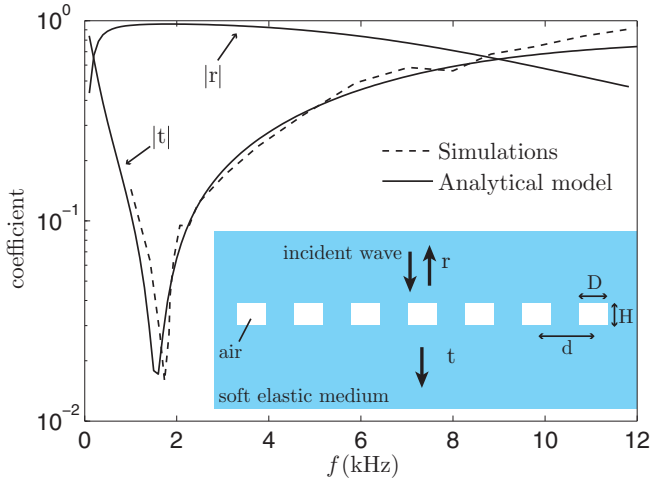
FIG. 1. (Color online) Comparison between Eq. (1b) and simulation data extracted from Fig. 16 in Ref. [20], for the transmission coefficient through a layer of air cylinders ($H = 2$ cm, $D = 1.5$ cm) on a square lattice ($d = 5$ cm) in silicone.

cylindrical cavities in silicone [20]. Hence, Eqs. (1) provide a reliable *analytic* expression for predicting the response of a bubble metascreen. The interest is twofold: An analytic formula allows one to identify the mechanisms involved in the response, and it also makes easier the analysis of the role of each parameter, in the perspective of an optimization process, for instance.

The strong coupling between the resonators is taken into account by the model with the two terms I and K. The first one is responsible for a slight shift in the resonance of the structure, which occurs at $\omega_0/\sqrt{I}$ instead of ω_0 for independent scatterers. The second one is crucial because it determines the way the metascreen couples to the longitudinal waves. Indeed, the term Ka that appears in Eqs. (1) can be interpreted as a superradiative damping term. When a bubble oscillates, it loses energy because of dissipation, but also because it radiates acoustic energy into the surrounding medium. For a single bubble, the corresponding damping term is ka. When N bubbles oscillate in phase, they radiate N times more intensely [23]. In a layer of bubbles, the number of bubbles coupled in phase with each other can be estimated by $N = (\lambda/d)^2$, where $\lambda = 2\pi/k$ is the wavelength. So Ka can be written as $Nka/(2\pi)$, i.e., a damping term proportional to N times the radiative damping of a single bubble. As the Minnaert resonance is at low frequency, N is large. For instance, in Fig. 1, $\lambda \simeq 70$ cm at minimum of transmission, which yields $N \simeq 200$ and $Ka \simeq 3$.

As illustrated in Fig. 1, a layer of bubbles is very efficient for blocking acoustic waves at frequencies close to the resonance frequency of the bubbles. However, one should not conclude that the incident energy is dissipated by the bubbles. At the minimum of transmission (i.e., for $\omega = \omega_0/\sqrt{I}$), Eq. (1a) predicts a reflection coefficient of $r = -Ka/(\delta + Ka)$. In general, $\delta \ll Ka$, which results in $r \simeq -1$: The bubble layer acts as a nearly perfect mirror.

From Eqs. (1), it is easy to show that the energy absorption of a layer of bubbles $A = 1 - |r|^2 - |t|^2$ is given, at the

minimum of transmission, by

$$A = \frac{2\delta Ka}{(\delta + Ka)^2}. \tag{2}$$

This expression indicates that an optimal absorption of $A = 1/2$ can be achieved if $\delta = Ka$. The dissipative damping factor includes two sources of losses: thermal and viscous. For cavities in a soft-elastic medium, the viscous losses generally dominate and are given by $\delta = 4\eta/(\rho a^2 \omega)$ [24], where η and ρ are the viscosity and density of the medium, respectively. One can thus define an optimal viscosity $\eta^\star = (\pi Z a^3)/(2d^2)$ for which the condition $\delta = Ka$ is satisfied (Z is the acoustic impedance of the medium). Interestingly, $\eta^\star$ does not depend on frequency, which means that the critical coupling can be satisfied for a wide frequency range.

Figure 2(a) shows the model predictions (lines) for a metalayer of $8-\mu$m-radius bubbles separated by $d = 50\ \mu$m in a soft solid characterized by $\mu = 1$ MPa, $Z = 1$ MRayl, and a viscosity of $\eta = \eta^\star = 0.32$ Pa s. Interestingly, the magnitudes of the reflection and transmission coefficients are close to 0.5 over an extended range of frequencies, not just at the resonance. This result comes from the fact that, as the resonator is overdamped, δ and Ka govern its response, and since both vary as the inverse of the frequency, the equality $Ka = \delta$ remains valid over a wide frequency range. Another consequence is that by changing the coupling
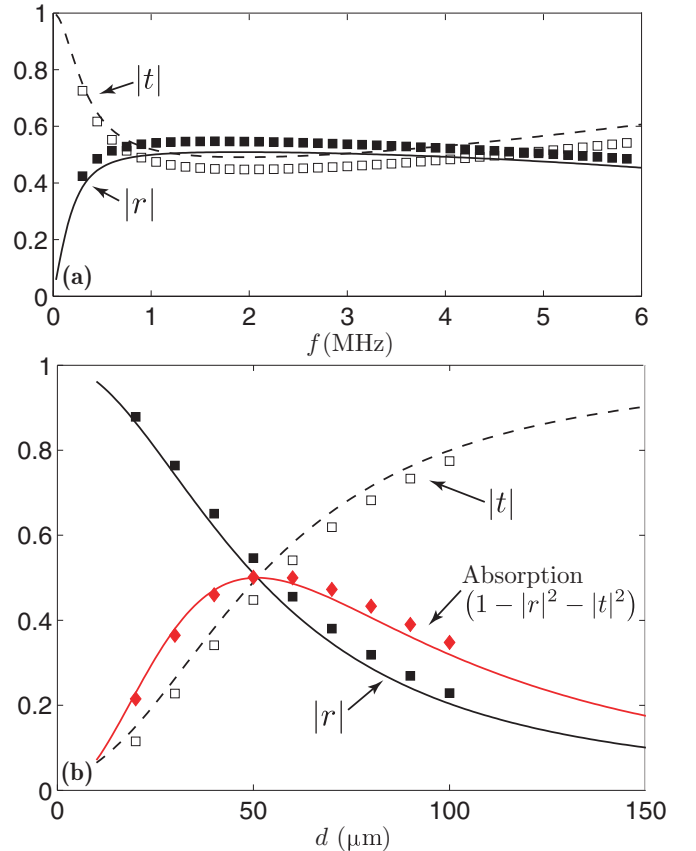

FIG. 2. (Color online) (a) Transmission and reflection predicted by the model (lines) and finite element simulations (symbols) for $\eta = \eta^\star$. (b) $|t|$, $|r|$, and absorption ($A = 1 - |r|^2 - |t|^2$) at 2 MHz as a function of bubble spacing d.

between the bubbles, one can tune the values of $|t|$ and $|r|$. This is illustrated in Fig. 2(b), where the magnitude of the transmission and reflection coefficients at 2 MHz (i.e., on the plateau) are reported as functions of the bubble spacing d. Thus, any value of $|t|$ between 0 and 1 can be achieved by choosing the proper spacing. Concentrated metascreens (small d) efficiently block transmission, whereas dilute metascreens (large d) are transparent. With the optimal spacing (50 μm here), the metascreen absorbs half of the energy, radiating the other half equally forward and backward. Finite element simulations were performed with cylindrical cavities with the same volume ($D = H = 14\ \mu$m), and good agreement was found (symbols in Fig. 2).

An interesting question is to determine whether the bubble metascreen is an acoustic equivalent of plasmonic devices encountered in optics. Indeed, its geometry and properties are reminiscent of the perforated metal films that lead to extraordinary optical transmission, for example. However, in plasmonics, the surface plasmon-polariton resonators do not couple directly to the incident propagating wave. To obtain the coupling, one needs to convert the propagating wave into an evanescent wave, which is usually done by the structure of the surface that acts as a diffraction grating. In our case, bubbles are natural low-frequency resonators that already couple efficiently with the incoming wave. The lattice of the screen does not play the role of a diffraction grating, rather, it controls the coupling between the bubbles. Thus, the analogy with plasmonics is not complete. Nevertheless, it is interesting to note that the bubble metascreens are perfectly described by the unified description proposed by Bliokh *et al.* [25], which is based on the open-resonator concept. Indeed, the bubble layer is an acoustic open resonator, with leakage and dissipative Q factors given by $Q_{\rm leak}^{-1} = Ka$ and $Q_{\rm diss}^{-1} = \delta$, respectively. Thus, it can be seen that the $\delta = Ka$ prescription for maximizing absorption is analogous to the so-called critical coupling condition in waveguide theory [26,27].

With a single metascreen, not more than half of the incoming energy can be absorbed. However, there is another situation in which a much larger absorption can be achieved: the case of a bubble metascreen close to a reflector, as depicted in the inset of Fig. 3(a). A simplified analysis of the total reflection by this structure considers only the interferences between the direct reflection from the bubble layer, and the multiple reflections between the layer and the reflector, which gives

$$r_{\rm tot} = r + \frac{t^2 r' \exp(2ikh)}{1 - rr' \exp(2ikh)}, \qquad (3)$$

where r' is the coefficient of the reflector and h the distance between the layer and the reflector. As shown on the right part of the inset of Fig. 3(a), the direct reflection from the bubbles brings a π shift, whereas the reflection from steel has a zero phase. As a consequence, there is destructive interference between the two paths. If h is small compared with the wavelength, the phase induced by the propagation over this distance can be neglected and the total reflection reduces to $r_{\rm tot} = (r + r' + 2rr')/(1 - rr')$, which is zero for $r = -r'/(1 + 2r')$.

In the case of a perfect reflector ($r' = 1$), one thus needs $r = -1/3$. Equation (1a) predicts that such a reflection coefficient is obtained for $\delta = 2Ka$, i.e., $\eta = 2\eta^\star$. Hence a
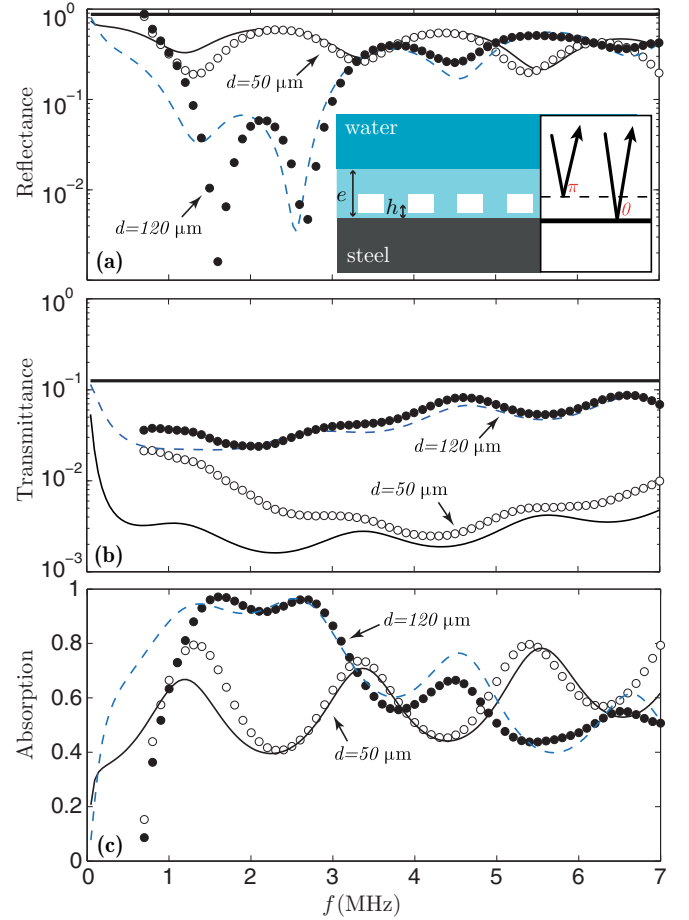

FIG. 3. (Color online) Experimental measurements (symbols) of the (a) reflectance, (b) transmittance, and (c) absorption for two different metascreens on a steel block. The solid thick horizontal lines are the values for the bare steel block. The solid and dashed lines show the prediction by the analytical model.

bubble metascreen with the proper bubble spacing should be able to transform a perfect reflector into a perfect absorber.

We have checked this prediction experimentally. Bubble metascreens were fabricated by soft lithography [17]: Cylindrical cavities of diameter $D = 24\ \mu$m and height $H = 13\ \mu$m ($a = 11\ \mu$m) were made in polydimethylsiloxane (PDMS), whose acoustic impedance was $Z = 1$ MRayl and rheological properties estimated from experiments to be $\mu = 0.6 + 0.7f$ MPa (f in MHz) and $\eta = 0.3$ Pa s [28]. With such parameters, superabsorption was predicted for a bubble spacing of $d = \sqrt{\pi Z a^2/\eta} = 118\ \mu$m. Two samples of the same thickness ($e = 230\ \mu$m) were made with different spacing: $d = 120$ and $50\ \mu$m. Acoustic experiments were performed by placing the cavities directly on a steel block ($h = H/2$) and measuring the reflection and transmission by standard ultrasonic techniques.

Figure 3 reports the parts of the energy that are reflected [Fig. 3(a)], transmitted [Fig. 3(b)], and absorbed [Fig. 3(c)]. For the steel block alone (thick horizontal lines), 88% of the energy is reflected and 12% transmitted. As expected, when the block is covered by the $d = 120\ \mu$m metascreen, the reflectance is drastically reduced [black circles in Fig. 3(a)], especially between 1.4 and 2.9 MHz, where less than 6%
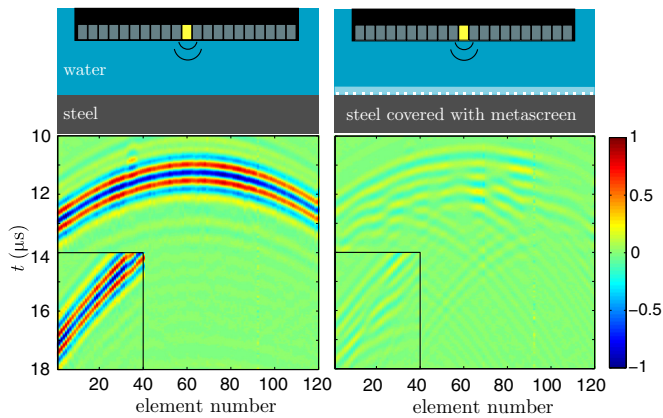
FIG. 4. (Color online) Pressure wave measured on each element of an array of transducers when a 2 MHz signal sent by an element in the middle is reflected either on the bare steel block (left) or on the same block covered with the optimized bubble metascreen (right). All the amplitudes are normalized by the maximum amplitude recorded in the bare block case. In the insets, the reflection of a tilted wave is recorded by emitting with the last element on the right.

of the energy is reflected, with the measured reflectance dropping nearly to zero at 1.6 MHz. Note that the oscillations in the measured coefficient are due to the extra reflection because of the impedance mismatch between PDMS and water. The model can take this extra reflection into account, and it captures well the experimental data. The importance of choosing the optimal bubble spacing is illustrated by the low reflectance reduction brought by the nonoptimized metascreen (white circles). Interestingly, the metascreens also reduce the transmission [Fig. 3(b)], the $d = 50 \ \mu$m sample having this time a smaller contribution. In terms of absorption [Fig. 3(c)], both metascreens manage to dissipate a significant part of the energy over a broad frequency range. The optimized metascreen shows very high absorption over the entire 1.4–2.9 MHz range, throughout which more than 91% of the incoming energy is dissipated, with a maximum absorbance of nearly unity at 1.6 MHz.

A further illustration of the performance of the metascreen is given in Fig. 4, which reports the measurements of the reflection of ultrasonic waves using an array of transducers. One element, in the middle of the array, emits a signal at 2 MHz and all the elements record the reflected wave. With the bare steel block (left part of Fig. 4), the reflected wave can be

clearly seen. But when the thin bubble metascreen is put onto the steel block, the wave is nearly invisible (right part of Fig. 4). The virtue of this configuration is the demonstration that the superabsorption is not limited to normal incidence: Even tilted waves can be absorbed. This is further demonstrated by the insets of Fig. 4 in which the 40 first elements record the wave emitted by the last element of the array (here the angle of incidence is of the order of $10°$).

A striking application of bubble metascreens is to make immersed objects invisible to sonar. In fact, many submarines are already equipped with anechoic coatings made of perforated soft solids. However, the optimization of such coatings is still an issue, which is usually tackled by numerical simulations. In the literature, the best reflectance reduction over the 8–22 kHz frequency range (relevant for sonar applications) was calculated at 22 dB by Ivansson for a 12-mm-thick rubber with bidisperse superellipsoidal inclusions [12]. As shown in the Supplemental Material [29], our analytical model predicts that a 35 dB reduction can be obtained with a 4-mm-thick metascreen, showing the advantage of our experimentally validated fully analytic approach.

In conclusion, we have shown how acoustic superabsorption can be achieved using a metascreen based on a periodic arrangement of bubbles embedded in a soft elastic matrix. Our analytical description provides a thorough understanding of the phenomenon and allows metascreens to be designed with fully tunable and optimized absorption properties over wide frequency ranges. This approach differs from methods based on iterative optimization, e.g., with genetic algorithms, and has the advantage of clearly identifying how the key material parameters (in our case, bubble size and separation, as well as matrix viscosity) should be adjusted to achieve optimized performance. Our approach has the merit of fully incorporating, and greatly benefiting from, the strong coupling between the local resonators, a point which is often neglected in metamaterials applications. This should therefore motivate the development of analogous methods, not only in acoustics but in optics, microwaves, and plasmonics as well.

[1] J. B. Pendry, Phys. Rev. Lett. **85**, 3966 (2000).

[2] R. A. Shelby, D. R. Smith, and S. Schultz, Science **292**, 77 (2001).

[3] J. Valentine, S. Zhang, T. Zentgraf, E. Ulin-Avila, D. A. Genov, G. Bartal, and X. Zhang, Nature (London) **455**, 376 (2008).

[4] S. Zhang, L. Yin, and N. Fang, Phys. Rev. Lett. **102**, 194301 (2009).

[5] D. Schurig, J. J. Mock, B. J. Justice, S. A. Cummer, J. B. Pendry, A. F. Starr, and D. R. Smith, Science **314**, 977 (2006).

[6] H. Chen and C. T. Chan, Appl. Phys. Lett. **91**, 183518 (2007).

[7] D. Torrent and J. Sánchez-Dehesa, New J. Phys. **10**, 023004 (2008).

[8] S. A. Cummer, B.-I. Popa, D. Schurig, D. R. Smith, J. Pendry, M. Rahm, and A. Starr, Phys. Rev. Lett. **100**, 024301 (2008).

[9] G. Lerosey, J. de Rosny, A. Tourin, and M. Fink, Science **315**, 1120 (2007).

[10] F. Lemoult, M. Fink, and G. Lerosey, Phys. Rev. Lett. **107**, 064301 (2011).

[11] N. I. Landy, S. Sajuyigbe, J. J. Mock, D. R. Smith, and W. J. Padilla, Phys. Rev. Lett. **100**, 207402 (2008).

[12] S. M. Ivansson, J. Acoust. Soc. Am. **124**, 1974 (2008).

[13] A. Moreau, C. Ciraci, J. J. Mock, R. T. Hill, Q. Wang, B. J. Wiley, A. Chilkoti, and D. R. Smith, Nature (London) **492**, 86 (2012).

[14] J. Mei, G. Ma, M. Yang, W. Wen, and P. Sheng, Nat. Commun. **3**, 756 (2012).

[15] G. Ma, M. Yang, S. Xiao, Z. Yang, and P. Sheng, Nat. Mater. **13**, 873 (2014).

[16] J. Christensen, V. Romero-Garcia, R. Pico, A. Cebrecos, F. J. Garcia de Abajo, N. A. Mortensen, M. Willatzen, and V. J. Sanchez-Morcillo, Sci. Rep **4**, 4674 (2014).

[17] V. Leroy, A. Bretagne, M. Fink, H. Willaime, P. Tabeling, and A. Tourin, Appl. Phys. Lett. **95**, 171904 (2009).

[18] E. Meyer, K. Brendel, and K. Tamm, J. Acoust. Soc. Am. **30**, 1116 (1958).

[19] D. C. Calvo, A. L. Thangawng, and C. N. Layman, J. Acoust. Soc. Am. **132**, EL1 (2012).

[20] A.-C. Hladky-Henion and J.-N. Decarpigny, J. Acoust. Soc. Am. **90**, 3356 (1991).

[21] S. M. Ivansson, J. Acoust. Soc. Am. **119**, 3558 (2006).

[22] V. Leroy, A. Strybulevych, M. G. Scanlon, and J. H. Page, Eur. Phys. J. E **29**, 123 (2009).

[23] C. Feuillade, J. Acoust. Soc. Am. **98**, 1178 (1995).

[24] A. Prosperetti, J. Acoust. Soc. Am. **61**, 17 (1977).

[25] K. Y. Bliokh, Y. P. Bliokh, V. Freilikher, S. Savel'ev, and F. Nori, Rev. Mod. Phys. **80**, 1201 (2008).

[26] Y. Xu, Y. Li, R. K. Lee, and A. Yariv, Phys. Rev. E **62**, 7389 (2000).

[27] C. Wu, B. Neuner, G. Shvets, J. John, A. Milder, B. Zollars, and S. Savoy, Phys. Rev. B **84**, 075102 (2011).

[28] V. Leroy, A. Strybulevych, J. H. Page, and M. G. Scanlon, Phys. Rev. E **83**, 046605 (2011).

[29] See Supplemental Material at http://link.aps.org/supplemental/10.1103/PhysRevB.91.020301 for details on the optimization.